Synthesis, characterization, and photoactivity of $InTaO_4$ and $In_{0.9}Ni_{0.1}TaO_4$ thin films prepared by electron evaporation

V. J. Rico
Instituto de Ciencia de Materiales de Sevilla, CSIC/Universidad de Sevilla, Avda. Americo Vespucio 49, 41092 Sevilla, Spain

F. Frutos
Departamento de Física Aplicada I, Universidad de Sevilla, Avenida Reina Mercedes s/n, 41012 Sevilla, Spain

F. Yubero, J. P. Espinos, and A. R. Gonzales-Elipe[a)]
Instituto de Ciencia de Materiales de Sevilla, CSIC/Universidad de Sevilla, Avda. Americo Vespucio 49, 41092 Sevilla, Spain

(Received 10 September 2009; accepted 16 November 2009; published 23 December 2009)

$InTaO_4$ and $In_{0.9}Ni_{0.1}TaO_4$ thin films have been prepared by electron evaporation of successive layers of the single oxide components and posterior annealing at $T>800$ °C. The annealed thin films presented the monoclinic crystallographic structure typical of these mixed oxides. The electrical and optical behaviors of the films, assessed by *C-V* measurements, surface conductivity as a function of temperature, and UV-vis absorption spectroscopy, indicate that these oxides are wide band gap semiconductors with a variable dielectric constant depending on the annealing conditions. By reflection electron energy loss spectroscopy some electronic states have been found in the gap at an energy that is compatible with the activation energy deduced from the conductivity versus $1/T$ plots for these oxides. The photoactivity of these materials has been assessed by looking to the evolution of the wetting contact angle as a function of the irradiation time. All the films became superhydrophilic when irradiated with UV light, while the $In_{0.9}Ni_{0.1}TaO_4$ thin films also presented a small partial decrease in wetting angle when irradiated with visible photons. © *2010 American Vacuum Society.* [DOI: 10.1116/1.3273597]

I. INTRODUCTION

Ta_2O_5 is a very well known dielectric material with many applications for the fabrication of different electrical devices.[1] This oxide is an insulator with a band gap of approximately 4.2 eV.[2,3] Another less well known property of this material is its ability to act as a photocatalyst,[4–6] although its practical use is restricted by the fact that photons of very short wave length (i.e., $\lambda<300$ nm) are required to photoinduce the generation of electron-hole pairs suitable to produce this type of photoactivation processes. Recently, new mixed oxides of the type $InTaO_4$ and $In_{0.9}Ni_{0.1}TaO_4$ (i.e., Ni-doped $InTaO_4$) have been claimed to be photoactive with visible light (i.e., with photons of $\lambda>400$ nm).[7] Owing to the large interest of these processes, different publications have recently reported about the synthesis, characterization, and analysis of these mixed oxides, particularly when they are prepared in the form of thin films.[8–12] However, a systematic investigation of their optical and electrical properties as a function of their microstructure is still missing. In the present work, we address the study of $InTaO_4$ and Ni-doped $InTaO_4$ thin films prepared by an electron evaporation physical vapor deposition process. To avoid the preferential evaporation of the single oxides from a mixed oxide target material, the films have been prepared by multiple sequential evaporation of Ta_2O_5, In_2O_3, and, in its case, Ni. After annealing at sufficiently high temperature, the multilayers of the individual thin films yield a single layer of the mixed oxides without any trace of the constituent single oxides. These final films have been characterized by different techniques including x-ray diffraction, UV-visible absorption spectroscopy, capacity-voltage measurements, x-ray photoemission spectroscopy (XPS), and reflection electron energy loss spectroscopy (REELS). These analyses confirm that both, $InTaO_4$ and $In_{0.9}Ni_{0.1}TaO_4$, thin films behave as wide band gap semiconductors very similar in their electronic properties to Ta_2O_5. The possibility that these materials can be photoactive with visible light is critically discussed by following the variation in the water contact angles on their surface when these films are illuminated with visible and UV light.

II. EXPERIMENT

A. Thin film preparation

Ta_2O_5 thin films have been prepared on quartz plates or Si (1 0 0) substrates at room temperature by electron evaporation under 10^{-4} torr of oxygen, using crucibles of 3 cm diameter. The films were thereafter annealed at increasing temperatures up to 1000 °C. Typical growing rates of 6 nm/min were used for the preparations. The mixed oxide thin films were prepared at room temperature in the same experimental setup where more than an oxide could be evaporated by automatically changing the crucible on which the electron

a)Electronic mail: arge@icmse.csic.es

beam impinges. Multilayer thin film oxides were prepared by successive evaporation of Ta_2O_5 (10 nm nominal thickness) and In_2O_3 (10 nm nominal thickness) layers. Up a maximum of 50 layers were deposited to reach a nominal thickness of 1000 nm for the $InTaO_4$ final films. In the case of the $In_{0.9}Ni_{0.1}TaO_4$ thin films (i.e., Ni doped indium tantalate) a similar procedure was used by including the evaporation of Ni (1 nm layers) in the multilayer sequence. To control the stoichiometry of the final mixed oxide films avoiding the segregation of single oxides grains, the evaporation rate of the single oxides was carefully calibrated by comparing the data of a quartz crystal monitor with the mass thickness of single oxide thin films determined by x-ray fluorescence and Rutherford backscattering. The as-prepared samples consisted of a mixture of the different oxides, but they were converted into the desired mixed oxides by annealing the multilayer films for 3 h at increasing temperatures up to 1000 °C.

B. Characterization methods

The optical properties of the samples were determined by UV-vis absorption spectroscopy in a Perkin-Elmer lambda 12 spectrometer for samples prepared on fused silica. Typical thickness of the samples used for optical characterization was around 350 nm.

Scanning electron microscopy (SEM) cross sections and normal images were measured in a Hitachi S5200 field emission microscope for thin films grown on a silicon wafer. The thickness of the samples for SEM analysis was of the order of 1 μm in most cases.

Structural characterization of the thin films was carried out by x-ray diffraction in a Siemens D5000 diffractometer working in the Bragg–Brentano configuration. The size of the crystalline domains was estimated by applying the Scherrer formula to the (1 1 0) peak of Ta_2O_5 (orthorhombic crystalline structure)[13] and the (−1 1 0) peak of the indium tantalate (monoclinic crystalline structure).[14]

Surface conductivity as a function of temperature was determined by a systematic study by two-probe direct current (dc) measurements in oxygen atmosphere over a temperature range of 600–200 °C. The dc measurements were carried out while cooling. The electrodes were fixed on the sample by applying silver paste on the surface of films. The measurements were carried out for the films deposited on polished *n*-type Si (1 0 0) wafers with an electrical resistivity of 1–5 Ω cm.

The capacitance-voltage (*C*-*V*) characteristics of the films were measured with a ESI2150-*LCR* apparatus. Capacitors were formed with Al contacts deposited by evaporation over a mask with 2×10^{-3} cm^2 holes to form metal-insulator-semiconductor (MIS) capacitors structures. The *C*-*V* curves of Al-oxide films-Si(*n*) capacitors were obtained by applying a small ac signal of 200 mV amplitude and 150 kHz and 100 Hz frequencies across the capacitor, while the direct current (dc) electric field was swept from negative bias to positive bias. The corresponding static permittivity of the films was determined from the accumulation capacitance (C_{ox}) of a MIS structure at 150 kHz.

From measurements of the response at high and low frequency capacitances, 150 kHz and 100 Hz, respectively, it is possible to associate the interface capacitance (C_{it}) with the density of traps D_{it} at the interface with the substrate,[15]

$$C_{it} = qD_{it}, \tag{1}$$

where

$$C_{it} = \left(\frac{1}{C_{LF}} - \frac{1}{C_{ox}}\right)^{-1} - \left(\frac{1}{C_{HF}} - \frac{1}{C_{ox}}\right)^{-1}, \tag{2}$$

and C_{LF}, C_{HF}, and C_{ox} are the capacitances a low and high frequencies and the capacitance of the bulk oxide.

XPS spectra were recorded on an Escalab 210 spectrometer working under energy transmission constant conditions. The Mg $K\alpha$ line was used for excitation of the spectra. They were calibrated in binding energy by referencing to the C 1*s* peak taken at 284.6 eV for the spurious carbon contaminating the surface of samples. Quantification was done by calculating the area of the peaks after correction with the sensitivity factor of each element. Reflection energy loss spectra were recorded in the same apparatus by exciting the spectra with an electron beam of 1500 or 500 eV supplied by a LEG-G2 electron gun. No significant differences in shape were observed for these two energies. The reported spectra were recorded with 1000 eV primary beam energy.

Bulk atomic ratio of the oxide was determined by x-ray fluorescence (XRF) in the SRS3000 x-ray spectrometer from Siemens. The anode consisted of a rhodium tube working at 3000 W of power. The analysis utilizes the bremsstrahlung emission as incident radiation. Semiquantitative evaluation of atom concentration was carried out with the software SPECTRA PLUS 1.5.4 by measuring the Lα1 peaks of Si, Ta, In, and Ni and by comparing the areas of the peaks after correction with their sensitivity factors.

Photoactivity of the samples was checked by measuring the water contact angles on illuminated surfaces of the different thin film samples. Illumination was carried out with a Xe lamp with photon intensity at the position of the samples of 2 W cm^{-2}. For simplicity we will refer to this situation in the text and figures as UV illumination. Other experiments consisted of the illumination with the same lamp by placing an UV filter between the lamp and the sample. The light intensity was then 1.6 W cm^{-2} at the sample position. In all cases an infrared filter (i.e., a water bath) was kept between the lamp and the samples to prevent any possible heating by the infrared radiation. From experiments with TiO_2 it is known that the wetting angle variation upon UV illumination is affected by the temperature of the film and the external humidity. In our case, we controlled the temperature of the holder during a complete illumination experiment and found that it did not change by more than 10 °C. All the experiments were carried out under similar conditions of the laboratory, so that no significant variations in ambient humidity were detected. Measurement of contact angle was carried out

by the Young method by dosing small droplets of de-ionized and bidistilled water on the surface of the illuminated samples. In the experiments where the contact angle variation was determined as a function of the illumination time, a metal foil acting as a shutter was used to close and open the lamp output. All wetting angle measurements within a given experiment were taken after illumination for successive periods of time. Therefore, the time scale in the plots refers to the accumulative illumination of the samples. The maximum uncertainty in the determination of the water contact angle is about 10°, depending on the sample position. In the course of this investigation it was noticed that the "as-prepared" thin films were more hydrophilic than the same samples a given time after their preparation. Therefore, storage conditions were carefully controlled by putting the samples in a desiccator until their use. The reported experiments were carried out with samples that have been stored for a sufficiently long period of time, so that they had stabilized their surface properties (the minimum time elapsed was 2 months since their preparation).

III. RESULTS

A. Thin film preparation and structural and microstructural characterization

Figure 1 shows a series of XRD diagrams for the tantalum oxide, indium tantalate, and Ni-doped indium tantalate thin films after annealing at 600, 800, and 1000 °C.[13,14] The diagrams of the original samples are not included because of their amorphous character. From these diagrams it is apparent that crystallization of Ta_2O_5 starts in a temperature range comprised between 600 and 800 °C. The crystallization of the monoclinic structure of the indium tantalate [cf. Fig. 1(b)] and Ni-doped indium tantalate [Fig. 1(c)] also takes place in this interval of temperature. This result indicates that interdiffusion of the different components occurs in this temperature range leading to the formation of the mixed oxide structure. It is worth noting that no peaks of the single oxides (i.e., Ta_2O_5 and In_2O_3) are observed after annealing at $T > 800$ °C, thus indicating that no segregated phases of these single oxides remain in the films after their annealing at the temperatures required to get the crystalline phases of these materials.[16] Annealing of the three samples at 1000 °C enhances their sintering and crystallization as evidenced by a drastic increase in the size of the crystalline domains at this temperature (Table I).

The annealing treatments also produce modifications in the microstructure of the films as evidenced by the SEM micrographs of the samples. Figure 2 shows cross section views of the three kinds of thin films as prepared and after annealing at 1000 °C. It is clear from these images that the annealing treatment produces a homogenization of the film microstructures. This homogenization is accompanied by the development of some voids due to contraction of the material.

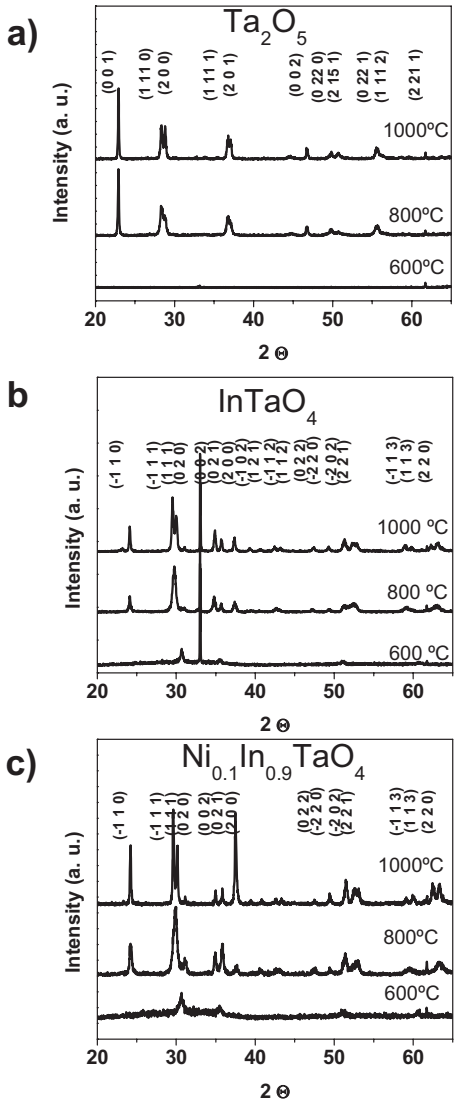

FIG. 1. XRD diagrams of Ta_2O_5 (a), $InTaO_4$ (b), and $Ni_{0.1}In_{0.9}TaO_4$ (c) annealed at the indicated temperatures. Attribution of the peaks to their corresponding diffraction planes is included in the figure.

B. Optical characterization of the films

Figure 3 shows the transmission spectra of the different thin films supported on quartz plates. They present the typical transmission spectra of a homogeneous thin film deposited on transparent substrates with a lower refraction index. These spectra are characterized by an oscillatory behavior due to the interference of the partially reflected light beams at the film-air and film-substrate interfaces. From the analysis of this interference pattern it is possible to obtain the thickness and the refraction index of the films. However, particularly for the films annealed at elevated temperatures, it is apparent an attenuation of the oscillations of the spectra and a decrease in the transmission at low wavelengths. These features can be associated with the scattering of light by the relatively large particles formed as a result of the sintering treatment at elevated temperatures. The modification of the spectral shape due to light scattering precludes the use of these spectra to obtain the refraction index or the band gap

TABLE I. Size of crystalline domains, proportions between the different cations, band gap energy evaluated by means of REELS, and dielectric constant and interface state density derived from the *C-V* curves.

Sample	Crystalline size (nm)	Cationic ratios (XPS and XRF)[a]	Band gap energy REELS (eV)	Dielectric constant	ISD (eV^{-1} cm^{-2})
Ta_2O_5 (800 °C)	55		···	28.7	5.2×10^{11}
Ta_2O_5 (1000 °C)	75		4.2	13.4	3.4×10^{10}
$InTaO_4$ (800 °C)	55	Ta/In=0.97	···	21.3	2.6×10^{11}
$InTaO_4$ (1000 °C)	63	Ta/In=1.15 (1.10)	4.6	14.1	1.7×10^{11}
$In_{0.9}Ni_{0.1}TaO_4$ (800 °C)	30	Ta/In=1.34 Ta/(In+Ni)=1.12	···	11.8	···
$In_{0.9}Ni_{0.1}TaO_4$ (1000 °C)	63	Ta/In=1.13 (1.24) Ta/(In+Ni)=0.78 (0.9)	4.6	6.5	···

[a]Data in parenthesis.

values of the films. Nevertheless, the position of the edge in the annealed films suggests that the band gap of these oxides must be higher than 4 eV.

C. Electronic characterization of the thin films

Approximate band gaps of the oxides can be obtained by REELS.[17] Since this technique has a surface character we have checked first by XPS that the composition and the chemical state of the elements of the mixed oxides correspond to those expected from their chemical formulas. Figure 4 shows a series of Ta 4*f*, In 3*d*, and Ni 2*p* spectra of the thin films annealed at 1000 °C. The spectral shape and binding energies (BEs) deduced from these spectra are, in all cases, typical of the Ta^{5+} (BE 31,0 eV), In^{3+} (BE 443,6 eV), and Ni^{2+} (BE 932,4 eV)[18] chemical states. In addition, the composition of the surface layers deduced from the intensity of these spectra yields the atomic ratios reported in Table I that are in good agreement with those expected from the chemical formula of the oxides and the values determined by XRF included in parenthesis in this table. The relatively good concordance between the two set of results supports that surface (i.e., XPS) and bulk composition (i.e., XRF) are quite similar and that, therefore, evidences in electronic structure obtained by XPS or REELS can be taken as representative of the bulk.

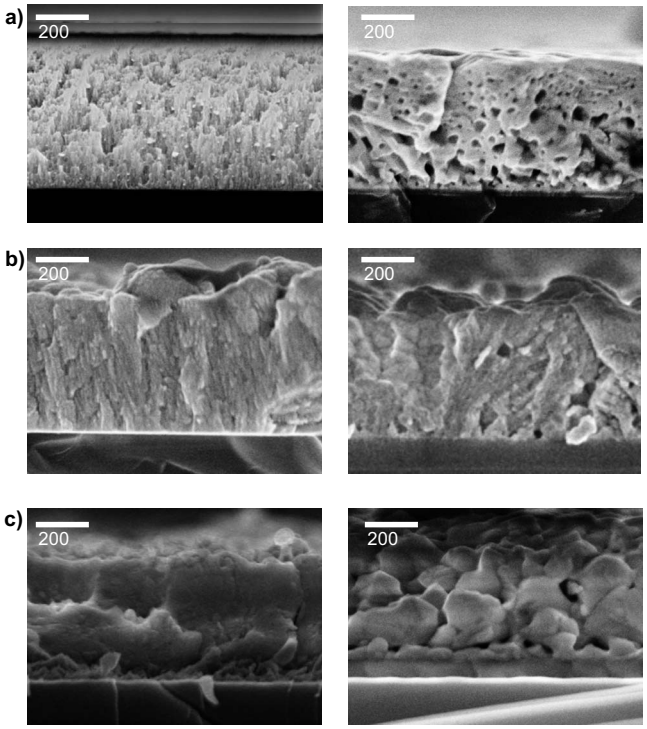

FIG. 2. SEM cross section micrographs of Ta_2O_5 (top), $InTaO_4$ (b), and $Ni_{0.1}In_{0.9}TaO_4$ (c) as prepared by electron evaporation (left) and after annealing at 1000 °C (right).

REELS spectra of the films annealed at 1000 °C are reported in Fig. 5. The spectra have been normalized to the intensity of the elastic peak (at the zero of the kinetic energy scale) and expanded in the *y* axis to clearly see the details around the band gap of the oxides. From these spectra, band gap energies have been determined by extrapolation to zero the edge jump at around 5 eV.[17] The obtained values, collected in Table I, indicate that the three oxides have a wide band gap that ranges from around 4.2 eV for Ta_2O_5 to 4.6 for $InTaO_4$ and $In_{0.9}Ni_{0.1}TaO_4$. Another interesting feature in these spectra is the existence of some losses in the gap region, as indicated by the asterisk included in the figure. In a previous publication on $InTaO_4$ thin films prepared by chemical vapor deposition,[11] similar states were detected with a higher intensity. In the present case the exact energy of these states cannot be determined accurately because their spectroscopic features overlap with the band corresponding to the elastic peak.

D. Dielectric properties of the films

C-V curves were recorded for Ta_2O_5, $InTaO_4$, and $Ni_{0.1}In_{0.9}TaO_4$ thin films annealed at 800 and 1000 °C. Figure 6 shows, as an example, the curves measured at 150 kHz and 100 Hz corresponding to the $InTaO_4$ thin films annealed

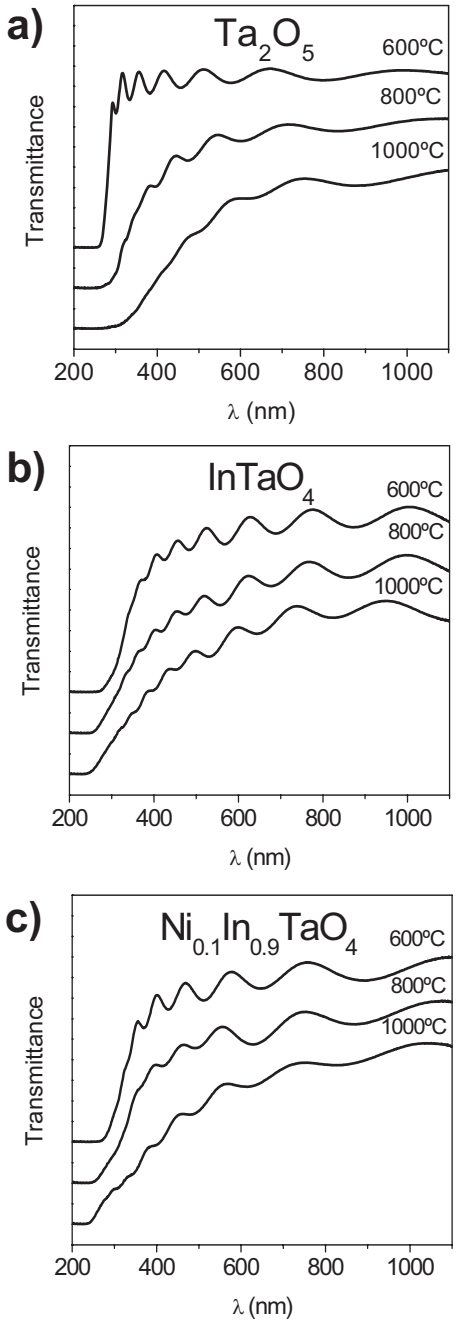

FIG. 3. UV-vis transmittance spectra of Ta_2O_5 (a), $InTaO_4$ (b), and $Ni_{0.1}In_{0.9}TaO_4$ (c) annealed at the indicated temperatures.

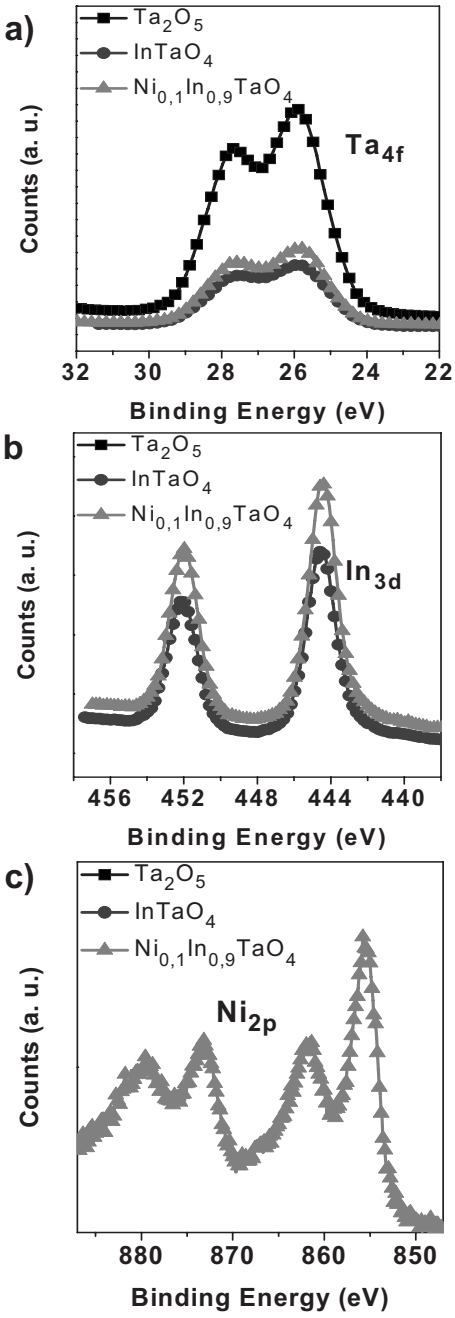

FIG. 4. Ta_{4f}, In_{3d}, Ni_{2p} core levels and valence band photoemission spectra of Ta_2O_5, $InTaO_4$, and $Ni_{0.1}In_{0.9}TaO_4$ annealed at the indicated temperatures.

at these two temperatures. The two curves present an accumulation region at $V>0$ with C values in the plateau that are different at 800 and 1000 °C. From the values of these plateaus and from the thickness of the layer determined by SEM, we have been able to derive the value of the effective dielectric constant of these thin film materials (i.e., 21.3 and 14.1 for the 800 and 1000 °C annealed films, respectively). Similar information was obtained from the other studied thin films and a summary of the effective dielectric constants is presented in Table I. The reported values show that the effective dielectric constants of the annealed films decrease when the annealing temperatures increase. This result agrees with the observation that the films coalesce and leave empty voids when annealed at 1000 °C (cf. Fig. 2). On the other hand, as deduced from the values of the minima in the interface state density (ISD) curves for $InTaO_4$ in Fig. 7, it can be concluded that after annealing at 1000 °C there is a decrease in the number of electronic traps at the interface with the substrate. A similar result is found for the two other materials and the obtained values are reported in Table I. Therefore, from the dielectric constant and the ISD values in Table I, it can be concluded that the films are quite insulator and that the annealing treatments at increasing temperatures contrib-

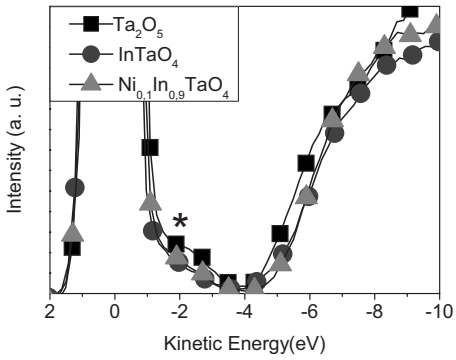

FIG. 5. REELS spectra represented in a expanded *y*-scale for Ta_2O_5, $InTaO_4$, and $Ni_{0.1}In_{0.9}TaO_4$ thin films annealed at 1000 °C.

ute to decrease the electronic states at the interface with the substrate. This latter is a well known phenomenon reported for other wide band gap semiconductors that has been related with an increase in the crystalline order of the film and the increase in the SiO_2 thickness at the interface as the annealing temperature increases.[19]

E. dc conductivity and activation energies

Surface conductivity measurements have been carried out as a function of temperature in the temperature range comprised between 600 and 200 °C. Figure 7 shows the obtained

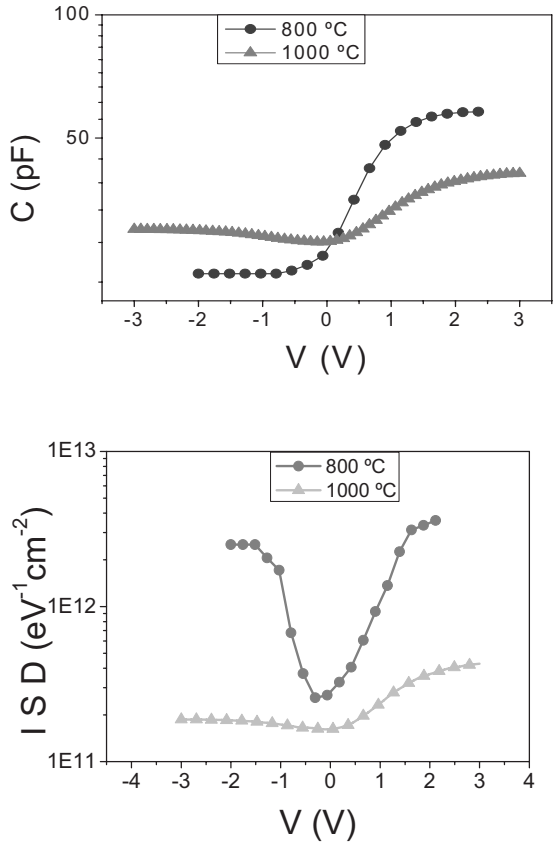

FIG. 6. (Top) *C-V* curves and (bottom) interface state density plots for $InTaO_4$ annealed at 800 and 1000 °C.

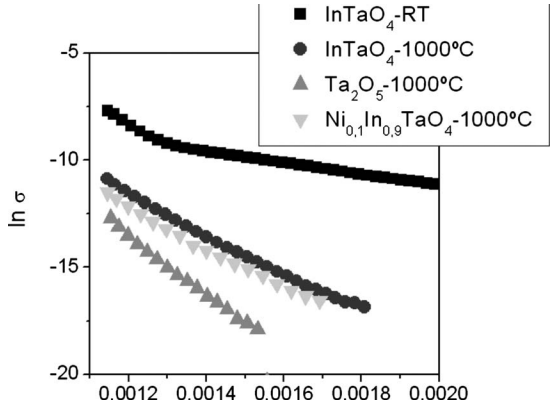

FIG. 7. Arrhenius plots of the dc conductivity of Ta_2O_5, $InTaO_4$, and $Ni_{0.1}In_{0.9}TaO_4$ annealed at the indicated temperatures. For comparison, the curve corresponding to the as-prepared $InTaO_4$ thin film is also included.

curves for the films annealed at 1000 °C. For comparison, the curve of the original $InTaO_4$ thin film before annealing (i.e., RT in the figure) is also included. In this case, its relatively high conductivity must be attributed to the presence in the film of unreacted and partially reduced indium oxide. Thus, the conductivity behavior of $InTaO_4$ annealed at 1000 °C confirms that no segregated In_2O_3 remains in the film after annealing. This behavior supports the previous results by XRD and XPS in the sense that annealing at $T > 800$ °C produces the interdiffusion of the two constituent oxides.

From the curves of the three annealed films, it is possible to estimate the activation energy of the conductivity process. From the Arrhenius plots in Fig. 7 the following activation energies were obtained: 0.9 eV for Ta_2O_5, 1.0 eV for $InTaO_4$, and 1.4 eV for Ni-doped $InTaO_4$. These values are also gathered in Table I. It is apparent from the graphs and these data that the samples only present slightly different values of conductivity and activation energies and that, in agreement with the relatively high values of their dielectric constants (cf. Table I), the three oxide thin films are very low electrical conductivity materials. It is interesting that the obtained activation energy values are compatible with the position of the shoulder determined by REELS for the three sets of thin films. We tentatively assume that they correspond to the same type of defects.

F. Light induced wetting behavior of the thin films

Water contact angle analysis of these thin films subjected to light irradiation showed that they depict photoactivity effects characterized by a decrease in the wetting angle up to a superhydrophilic state (i.e., wetting angle smaller than 10°). Figure 8 shows a series of plots of the water contact angle on the three thin films annealed at 1000 °C. The measurements were done for the films illuminated for increasing periods of time first with visible light and then with the whole range of wavelengths provided by the Xe lamp. It is apparent that the water contact angle does not vary when Ta_2O_5 is illuminated with visible light, although a drastic decrease up to a com-

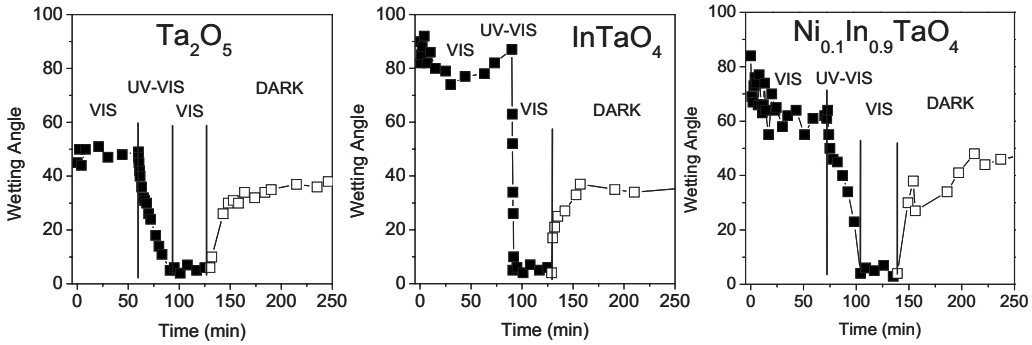

FIG. 8. Evolution of the water contact angle on the surface of Ta_2O_5, $InTaO_4$, and $Ni_{0.1}In_{0.9}TaO_4$ thin films annealed at 1000 °C illuminated first with visible and then UV lights. The recovery of the wetting angle in the dark is also shown.

plete hydrophilic state is found when the films are illuminated with UV light. This behavior has been previously discussed by assuming that illuminating this wide band gap semiconductor with light of the appropriate wavelength (i.e., $E_{hv} > E_g$, this latter the energy of the band gap of the material) produces the generation of couples of electrons-holes that migrating toward the surface produce some surface reactions leading to the hydrophilic conversion of the material.[4] Although some controversy exists on this topic, the most generally accepted explanation assumes that new –OH groups are produced on the surfaces of these oxides by their illumination under ambient conditions.[20] $InTaO_4$ and $In_{0.9}Ni_{0.1}TaO_4$ present a similar behavior than Ta_2O_5, although in the case of the Ni-doped $InTaO_4$ thin films there was a slight decrease in wetting angle when it was illuminated with visible light. This latter tendency has been discussed by us for other systems and attributed to the presence of some electronic states close to the surface that can be activated with visible light.[11] In this way, photons with an energy smaller than E_g result effective for promoting a partial hydrophilic conversion of the surface. The highly hydrophilic state reached for the three materials after UV illumination is maintained as long as the surface is illuminated, but evolves toward the initial state when the thin films are kept in the dark. A similar result was found on TiO_2 and N-doped TiO_2 thin films where these properties have been mostly studied.[12,20,21] Most common explanation of this behavior assumes the modification of the hydroxylation state of the surface due to the relaxation of their surface planes.

IV. DISCUSSION

In the present work we have developed a new strategy for the preparation of mixed oxide thin films by the successive evaporation of very thin layers of the constituent single oxides followed by the annealing of the films at elevated temperature. The XRD analysis of the final films annealed at $T > 800$ °C confirms that no segregated phases of the constituent oxides remain in the films and that, therefore, a complete solid state reaction to yield the mixed oxides has taken place at those temperatures. XPS analysis of the surface of the films confirms that, within the experimental errors, their stoichiometric correspond (or it is very close) to their theoretical formulas. Therefore, we can assume that the analysis of the electronic and electrical properties of the films refers to the mixed oxides with the desired compositions.

The REELS characterization of the mixed oxide thin films has shown that the three materials are wide band gap semiconductors with a band gap comprised between 4.2 and 4.6 eV. The obtained value for Ta_2O_5 agrees well with those determined for by other more accurate methods.[2,3] On the other hand, the electrical behavior of the three oxides is also typical of dielectric materials. Thus, the values obtained for their dielectric constant, particularly after annealing at 800 °C, are typical of high dielectric materials. The diminution in the value of this parameter obtained after annealing at 1000 °C is likely due to the formation of big particles by sintering. According to the SEM micrographs in Fig. 2 this process produces a series of voids in the films that contribute to decrease the value of the dielectric constant. By contrast, the annealing treatments at the highest temperatures produce a decrease in the interface state density, likely due to healing processes occurring under these conditions. This behavior is typical of low conductive oxides annealed in oxygen.[19]

On the other hand, the dielectric character of the films is confirmed by the analysis of dc their conductivity as a function of temperature. The curves in Fig. 7 indicate that the three oxide thin films have a very low conductivity. The value of the conductivity activation energy varies between 0.9 and 1.4 eV, probably indicating that conductivity is controlled by the electron activation from electronic states in the gap separated by this magnitude from the valence band. It is likely that these states correspond to the features detected by REELS between 1 and 2 eV (cf. Fig. 5).

The three oxides present a similar wetting behavior upon light irradiation characterized by the conversion of their surface state from partially hydrophobic into superhydrophilic (i.e., wetting angles lower than 10°). Only the $In_{0.9}Ni_{0.1}TaO_4$ thin film presents a slight decrease in wetting angle when illuminated with visible light. However, this behavior does not necessarily imply that this oxide is fully photoactive in the visible. According to recent investigations on N-doped TiO_2,[12,20] surface visible photoactivity effects can be induced by the excitation of defect states on the surface of the oxides. In this way electron and holes can be produced in regions

close to the surface where, after reaction with surface species, they would lead to the superhydrophilic state. We tentatively relate these states with the electronic defects around 1–2 eV detected by REELS on this oxide (cf Fig. 5).

In conclusion, the most important evidence from our investigation is that the three oxides are wide band gap semiconductors which are able to convert their surface into superhydrophilic when they are illuminated with UV light. However, none of these oxides present a defined photoactivity with visible light capable of making their surface superhydrophilic or photocatalytically active. This behavior is in contrast with previous reports in the literature in the sense that Ni-doped $InTaO_4$ oxide can be photoactive with visible light.[7]

ACKNOWLEDGMENTS

The authors thank the Ministry of Science and Education of Spain (Project No. MAT 2007-65764 and the CONSOLIDER INGENIO 2010-CSD2008-00023) and the Junta de Andalucia (Project Nos. TEP2275 and P07-FQM-03298) for financial support.

[1]C. Chaneliere, J. L. Autran, R. A. B. Devine, and B. Balland, Mater. Sci. Eng. R. **22**, 269 (1998).
[2]J. M. Albella, J. M. Martinez-Duart, and F. Rueda, Opt. Acta **22**, 973 (1975).
[3]T. Babeva, E. Atanassova, and J. Koprinarova, Phys. Status Solidi A **202**, 330 (2005).
[4]V. Rico, A. Borrás, F. Yubero, J. P. Espinós, F. Frutos, and A. R. González-Elipe, J. Phys. Chem. C **113**, 3775 (2009).
[5]Y. Zhu, F. Yu, Yi Man, Q. Tian, Y. He, and N. Wu, J. Solid State Chem. **178**, 224 (2005).
[6]T. Sreethawong, S. Ngamsinlapasathian, Y. Suzuki, and S. Yoshikawa, J. Mol. Catal. A: Chem. **235**, 1 (2005).
[7]Z. Zou, J. Ye, K. Sayama, and A. Arakawa, Nature (London) **414**, 625 (2001).
[8]H. C. Chen, H. C. Chou, J. C. S. Wu, and H. Y. Lin, J. Mater. Res. **23**, 1364 (2008).
[9]H. Kawakami and K. Maki, Vacuum **82**, 95 (2007).
[10]K. Maruta, H. Kawakami, and K. Maki, Jpn. J. Appl. Phys., Part 1 **46**, 774 (2007).
[11]N. McSporran *et al.*, Surf. Coat. Technol. **201**, 9365 (2007).
[12]A. Borrás *et al.*, J. Phys. Chem. C **111**, 1801 (2007).
[13]J. Roth, Solid State Chem. **2**, 445 (1970).
[14]J. Liebertz, Acta Crystallogr., Sect. B: Struct. Crystallogr. Cryst. Chem. **28**, 3100 (1972).
[15]E. H. Nicollian and J. R. Brews, *MOS Physics and Technology* (Wiley, New York, 1982), pp. 319–353.
[16]Z. Zou, J. Ye, and A. Arakawa, Chem. Phys. Lett. **332**, 271 (2000).
[17]F. Yubero, V. M. Jiménez, and A. R. González-Elipe, Surf. Sci. **400**, 116 (1998).
[18]C. D. Wagner, W. M. Riggs, L. E. Davis, and J. F. Moulder, *Handbook of X-Ray Photoelectron Spectroscopy* (Pelkin Elmer, Eden Prairie, MN, 1979).
[19]S. Duenas *et al.*, Semicond. Sci. Technol. **20**, 1044 (2005).
[20]R. Wang, K. Hashimoto, A. Fujishima, M. Chikuni, E. Kojima, A. Kitamura, M. Shimohigoshi, and T. Watanabe, Nature (London) **388**, 431 (1997).
[21]P. Romero-Gómez, V. Rico, A. Borrás, A. Barranco, J. P. Espinós, J. Cotrino, and A. R. González-Elipe, J. Phys. Chem. C **113**, 13341 (2009).